

## Article

# Expanding the Chemical Diversity of *Stemona parviflora*: Isolation and Characterization of New Parvistemoline-Type Alkaloids

Shuaizhen Zhou <sup>1</sup> , Ruolin Geng <sup>2,3</sup>, Changqiang Ke <sup>1,3</sup>, Fan Ge <sup>1</sup>, Ying Chen <sup>3,4</sup>, Chunping Tang <sup>1,3,\*</sup>  and Yang Ye <sup>1,2,3,4,\*</sup> 

- <sup>1</sup> State Key Laboratory of Drug Research, Shanghai Institute of Materia Medica, Chinese Academy of Sciences, Shanghai 201203, China; zhoushuaizhen@sibcb.ac.cn (S.Z.); kechangqiang@simm.ac.cn (C.K.); fange99@126.com (F.G.)
- <sup>2</sup> School of Chinese Materia Medica, Nanjing University of Chinese Medicine, Nanjing 210023, China; gengruolin@simm.ac.cn
- <sup>3</sup> China-Serbia “Belt and Road” Joint Laboratory for Natural Products and Drug Discovery, Shanghai Institute of Materia Medica, Chinese Academy of Sciences, Shanghai 201203, China; chenying1@simm.ac.cn
- <sup>4</sup> University of Chinese Academy of Sciences, No. 19A Yuquan Road, Beijing 100049, China
- \* Correspondence: tangcp@simm.ac.cn (C.T.); yye@simm.ac.cn (Y.Y.)

**Abstract:** A comprehensive phytochemical investigation of the whole plant of *Stemona parviflora* led to the isolation of 13 alkaloidal constituents, including five new alkaloids, parvistemonines B–F (1–5). The structures of these compounds were elucidated through extensive analyses of 1D and 2D NMR spectra, DFT NMR calculation, and comparisons with data in the literature. Notably, compounds 1–4 represent new examples of the rare parvistemoline-type alkaloids, with compound 4 showcasing a unique rearranged skeleton. Additionally, parvistemonine F (5) was identified as a distinct alkaloid skeleton characterized by a *n*-butyl side chain. These findings significantly expand our understanding of the chemical diversity of parvistemoline-type alkaloids and provide clues for elucidating the biosynthetic pathways of these structurally unique parvistemoline alkaloids.

**Keywords:** *Stemona parviflora*; alkaloid; parvistemoline-type; parvistemonines B–F



Academic Editor: George Grant

Received: 14 December 2024

Revised: 8 January 2025

Accepted: 10 January 2025

Published: 13 January 2025

**Citation:** Zhou, S.; Geng, R.; Ke, C.; Ge, F.; Chen, Y.; Tang, C.; Ye, Y. Expanding the Chemical Diversity of *Stemona parviflora*: Isolation and Characterization of New Parvistemoline-Type Alkaloids. *Chemistry* **2025**, *7*, 6. <https://doi.org/10.3390/chemistry7010006>

**Copyright:** © 2025 by the authors. Licensee MDPI, Basel, Switzerland. This article is an open access article distributed under the terms and conditions of the Creative Commons Attribution (CC BY) license (<https://creativecommons.org/licenses/by/4.0/>).

## 1. Introduction

Stemonaceae is a small family of monocotyledonous flowering plants within the order Pandanales, consisting of four genera: *Croomia*, *Stemona*, *Stichoneuron*, and *Pentastemona*, with about 37 known species [1,2]. These plants are native to Southeast Asia, Northern Australia, China, Japan, and Northern America [1,3]. *Stemona* is the largest genus, with approximately 25–32 species, known for its unique alkaloids, which typically feature either a pyrrolo- or a pyrido[1,2- $\alpha$ ]azepine core. To date, over 250 alkaloids of various structural types have been isolated from different *Stemona* species, with previous research demonstrating that these alkaloids exhibited various biological activities such as antitussive, insecticidal, antifeedant, nematocidal, and repellent properties [4,5].

*Stemona parviflora* C. H. Wright is a species endemic mostly in Hainan and Guangdong Province, China [6]. It has a long-standing history of use in Chinese folk medicine, commonly referred to as “Baibu”, where it is employed to treat respiratory disorders, including pulmonary tuberculosis and bronchitis, as well as for its insecticidal properties [6]. Despite its traditional uses, there have been relatively few chemical investigations into this

species in recent years [7–13]. These studies revealed the existence of minor phenylethyl benzoquinones and phenanthrenes in addition to the predominant alkaloids. A unique structural type of alkaloid, belonging to the parvistemoline group [14,15], has been identified in this species. This group, with only 13 derivatives reported so far, is characterized by the presence of a substituent at the C-9 position of the pyrrolo[1,2- $\alpha$ ]azepine nucleus and the absence of a fused B-C ring system, which distinguishes it from other groups of *Stemona* alkaloids [5]. This limited exploration underscores the need for further research into this species.

This investigation aims to explore and identify new alkaloidal constituents from *S. parviflora*, thereby providing valuable insights into its phytochemical profile and potential therapeutic applications. A systematic chemical investigation was conducted, resulting in the isolation of a total of 13 alkaloids, including four novel parvistemoline-type compounds (1–4, Figure 1), one new stemofoline-type derivative (5, Figure 1), and eight known compounds. The structures of these compounds were elucidated through extensive analysis of spectroscopic data, including MS, IR, and 1D and 2D NMR spectroscopic data and density functional theory (DFT) NMR calculations, as well as comparisons with existing literature.

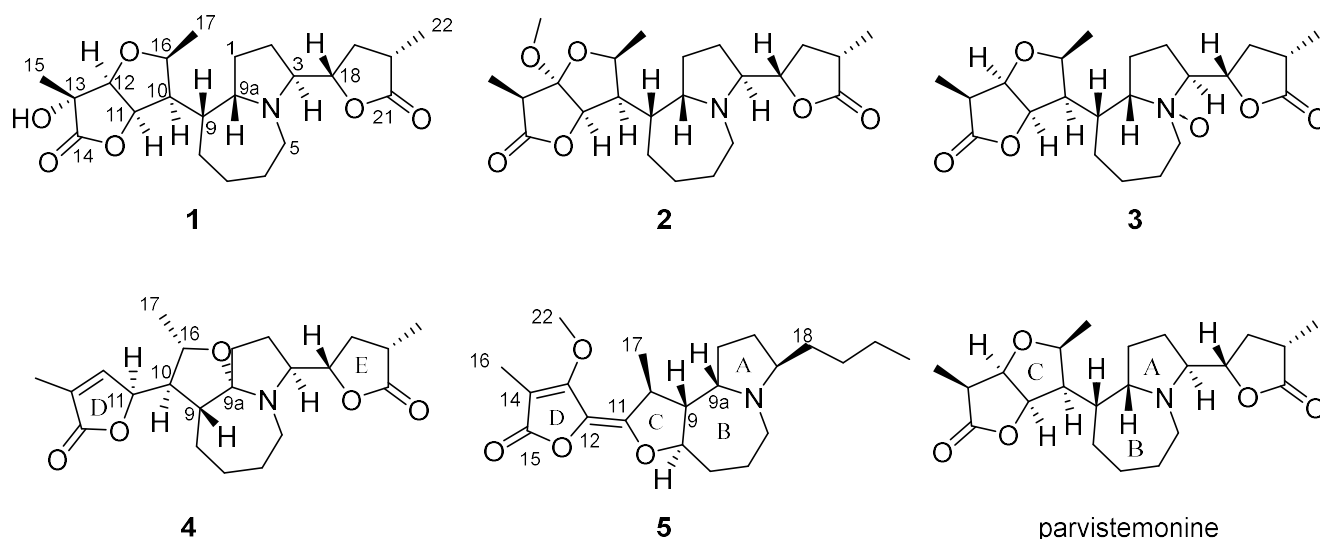


**Figure 1.** Structures of compounds 1–5 and parvistemonine.

## 2. Materials and Methods

### 2.1. General Experimental Procedures

Optical rotations were measured with a Perkin-Elmer 241MC polarimeter (PerkinElmer, Waltham, MA, USA) or a Perkin-Elmer 341 polarimeter (PerkinElmer, Waltham, MA, USA). IR spectra were recorded using a Perkin-Elmer 577 Spectrometer (PerkinElmer, Waltham, MA, USA). ESIMS were measured by using a Finnigan LCQ-DECA mass spectrometer (Thermo Fisher Scientific, San Jose, CA, USA) and HRESIMS were obtained on a Waters Q-TOF Micro MS spectrometer (Waters Corporation, Milford, MA, USA). EIMS and HREIMS were recorded on a Finnigan MAT-95 mass spectrometer (Thermo Fisher Scientific, San Jose, CA, USA).  $^1\text{H}$ ,  $^{13}\text{C}$ , and 2D NMR spectra were recorded on a Bruker AM-300 (Bruker Corporation, Bremen, Germany), Varian INOVA 400 (Agilent Technologies, Santa Clara, CA, USA) or Bruker Avance III 500 NMR spectrometer (Bruker Corporation, Billerica, MA, USA) with solvent resonances ( $\text{CDCl}_3$ ,  $\delta_{\text{H}}$  7.26;  $\delta_{\text{C}}$  77.16) as internal standards. Chemical shifts were reported in ppm ( $\delta$ ), with coupling constants ( $J$ ) in hertz. Column chromatographic separations were carried out using silica gel (Qingdao Haiyang Chemical Group Corporation, Qingdao, China) and Sephadex LH-20 (Pharmacia Biotech AB, Uppsala, Swe-

den) as packing materials. Precoated silica gel 60 F<sub>254</sub> aluminum sheets (Merck Millipore, Darmstadt, Germany) were used for analytical TLC. Visualization of TLC spots was performed by Dragendorff's reagent and Iodine. Analytical HPLC was performed on a Waters 2695 separations module coupled with a Waters 998 DAD UV detector (Waters Corporation, Milford, MA, USA), a Waters Acquity<sup>®</sup> ELSD (Waters Corporation, Milford, MA, USA), and a Waters 3100 SQD MS (Waters Corporation, Milford, MA, USA). The HPLC-MS analyses were performed on a Waters Sunfire<sup>®</sup> (Waters Corporation, Milford, MA, USA) RP C<sub>18</sub>, 3.5 μm, 4.6 × 100 mm column using a gradient solvent system composed of H<sub>2</sub>O and CH<sub>3</sub>CN (5% to 95%) with 0.1% formic acid at a flow rate of 1.0 mL/min.

## 2.2. Plant Material

Whole plants of *S. parviflora* were collected in Hainan province, China in 2013 and identified by Professor Jin-Gui Shen from the Shanghai Institute of Materia Medica, Chinese Academy of Sciences. A voucher specimen (No. 20130401) has been deposited in the Herbarium of the Shanghai Institute of Materia Medica, Chinese Academy of Sciences.

## 2.3. Extraction and Isolation

Air-dried roots of *S. parviflora* (10.0 kg) were grounded into powder and extracted with 95% EtOH (25 L) three times, for three days each. After the evaporation of the collected filtrate, the crude extract was acidified with dilute HCl (4%) to pH 1–2 and partitioned between ethyl ether and water. The aqueous part was basified with aqueous NH<sub>3</sub> to pH 9–10 and extracted repeatedly with CH<sub>2</sub>Cl<sub>2</sub> to afford 70 g of crude alkaloid. The crude alkaloid was subjected to column chromatography over silica gel (200–300 mesh) and eluted with petroleum ether–acetone from 4:1 to 1:4, and then acetone to yield four major fractions (XB1–XB4). Fraction XB1 was subjected to repeated column chromatography over silica gel and then Sephadex LH-20 to afford isomaistemone (151 mg), maistemone (49 mg), and croomine (553 mg). Similarly, fraction XB2 gave parvistemonine C (2, 515 mg), parvistemonine F (5, 64 mg), parvineostemonine (143 mg), and parvistemonine (4.9 g) and fraction XB3 afforded parvistemonine B (1, 832 mg), parvistemonine D (3, 2 mg), parvistemonine E (4, 64 mg), protostemonine (533 mg), and protostemoamide (5 mg). Stemofoline (680 mg) was afforded from fraction XB4.

### 2.3.1. Parvistemonine B (1)

Light yellow amorphous powder;  $[\alpha]_D^{20} + 4$  (c 0.1, MeOH); IR (KBr)  $\nu_{\max}$  3432, 2935, 1770, 1664, 1456, 1380, 1195, 1088, 1016, and 939 cm<sup>-1</sup>; <sup>1</sup>H and <sup>13</sup>C NMR data: see Tables 1 and 2; EIMS  $m/z$ : 407 [M]<sup>+</sup>, 308 (100) [M – 99]<sup>+</sup>; HREIMS  $m/z$ : 407.2305 [M]<sup>+</sup> (calcd for C<sub>22</sub>H<sub>33</sub>NO<sub>6</sub>, 407.2308).

### 2.3.2. Parvistemonine C (2)

Yellow amorphous powder;  $[\alpha]_D^{20} + 81$  (c 0.1, Acetone); IR (KBr)  $\nu_{\max}$  2935, 1787, 1776, 1456, 1381, 1190, 1041, 991, and 754 cm<sup>-1</sup>; <sup>1</sup>H and <sup>13</sup>C NMR data: see Tables 1 and 2; EIMS  $m/z$ : 421 [M]<sup>+</sup>, 322 (100) [M – 99]<sup>+</sup>; HRESIMS  $m/z$ : 422.2544 (calcd for C<sub>23</sub>H<sub>36</sub>NO<sub>6</sub>, 422.2543).

### 2.3.3. Parvistemonine D (3)

Yellow amorphous powder;  $[\alpha]_D^{20} + 9$  (c 0.1, MeOH); IR (KBr)  $\nu_{\max}$ : 3433, 2937, 1772, 1457, 1167, 997 cm<sup>-1</sup>; HRESIMS  $m/z$ : 408.2385 (calcd for C<sub>22</sub>H<sub>34</sub>NO<sub>6</sub>, 408.2386). <sup>1</sup>H-NMR (300 MHz, CDCl<sub>3</sub>):  $\delta_H$  4.91 (dd, 1H,  $J = 3.8, 3.9$  Hz; H-11), 4.61 (m, 1H; H-12), 4.32 (m, 1H; H-16), 4.05 (m, 1H; H-18), 3.85 (m, 1H; H-5 $\beta$ ), 3.70 (m, 3H; H-3, H-5 $\alpha$ , and H-9a), 2.70 (m, 3H; H-13, H-19, and H-20), 2.50 (m, 1H; H-9), 2.20–1.50 (m, 10H; H-1, H-2, H-6, H-7, and H-8), and 1.30 (m, 9H; Me-15, Me-17, Me-22); <sup>13</sup>C-NMR (100 MHz, CDCl<sub>3</sub>):  $\delta_C$  24.8 (t, C-1);

24.1 (t, C-2), 76.9 (d, C-3), 69.0 (t, C-5), 23.5 (t, C-6), 26.7 (t, C-7), 28.1 (t, C-8), 34.9 (d, C-9), 73.9 (d, C-9a), 49.7 (d, C-10), 89.6 (d, C-11), 79.8 (d, C-12), 41.2 (d, C-13), 178.2 (s, C-14), 18.6 (C-15), 77.1 (d, C-16), 9.0 (q, C-17), 83.0 (d, C-18), 34.8 (t, C-19), 34.2 (d, C-20), 178.5 (s, C-21), and 14.9 (q, C-22). The signals were assigned according to the proton and carbon assignments of the known compound parvistemonine.

**Table 1.**  $^1\text{H}$  NMR data (300 MHz) for compounds **1**, **2**, and **4** in  $\text{CDCl}_3$ .

No.	1	2	4
1	1.42, m 1.64, m	1.40, m 1.64, m	1.67, m 1.90, m
2	1.59, m 1.75, m	1.59, m 1.75, m	1.42, m 2.05, m
3	3.45, m	3.40, m	3.16, m
5	2.87, dd (15.7, 11.9) 3.40, m	2.85, d (11.7) 3.30, dd (11.7, 7.9)	2.99, dd (14.4, 11.4) 2.74, d (14.4)
6	1.44, m 1.72, m	1.42, m 1.70, m	1.59, m 1.65, m
7	1.42, m; 1.82, m	1.38, m 1.77, m	1.42, m; 1.61, m
8	1.46, m; 1.92, m	1.45, m 1.91, m	1.60, m 1.71, m
9	2.18, m	2.15, m	2.38, m
9a	3.45, m	3.43, m	
10	2.15, m	2.30, m	2.01, m
11	5.14, d (3.8)	4.61, d (4.3)	4.84, dd (3.4, 1.7)
12	4.25, d (3.8)		7.02, d (1.7)
13		2.89, m	
15	1.50, s, 3H	1.34, d (7.2)	1.92, s
16	4.30, m	4.48, m	3.55, m
17	1.15, d (6.7), 3H	1.20, d (6.6)	1.28, d (5.9)
18	4.20, m	4.17, ddd (10.8, 7.1, 5.3)	4.22, m
19	1.55, m 2.37, m	1.55, m 2.35, m	2.36, m 1.49, m
20	2.61, m	2.59, m	2.62, m
22	1.25, d (7.1), 3H	1.25, d (7.0), 3H	1.24, d (7.0), 3H
23-OMe		3.35, s, 3H	

**Table 2.**  $^{13}\text{C}$  NMR data (125 MHz) for compounds **1**, **2**, and **4** in  $\text{CDCl}_3$ .

No.	1	2	4
1	27.0 t	27.1 t	38.6 t
2	26.8 t	26.9 t	23.7 t
3	63.7 d	63.7 d	67.0 d
5	46.5 t	46.6 t	46.0 t
6	24.5 t	24.8 t	23.1 t
7	28.6 t	28.7 t	31.2 t
8	26.7 t	26.9 t	27.0 t
9	39.1 d	39.0 d	46.5 d
9a	62.8 d	62.9 d	105.1 s
10	49.4 d	47.4 d	50.3 d
11	84.0 d	86.4 d	80.9 d
12	84.4 d	110.3 s	147.3 d
13	76.1 s	44.7 d	130.6 s
14	177.6 s	176.3 s	173.8 s
15	18.6 q	10.0 q	10.8 q

Table 2. Cont.

No.	1	2	4
16	77.9 d	79.4 d	71.3 d
17	19.3 q	19.4 q	20.2 q
18	83.3 d	83.4 d	82.2 d
19	34.2 t	34.2 t	33.7 t
20	34.9 d	35.0 d	35.4 d
21	179.8 s	179.7 s	179.9 s
22	14.9 q	15.0 q	15.2 q
23-OMe		51.2 q	

## 2.3.4. Parvistemonine E (4)

Light yellow amorphous powder;  $[\alpha]_D^{20} - 4$  (c 0.2, Acetone); IR (KBr)  $\nu_{\max}$  2929, 1759, 1668, 1456, 1334, 1163, and 754  $\text{cm}^{-1}$ ;  $^1\text{H}$  and  $^{13}\text{C}$  NMR data: see Tables 1 and 2; ESI-MS  $m/z$ : 390.4  $[\text{M} + \text{H}]^+$ , EIMS  $m/z$  389  $[\text{M}]^+$ , 290 (100)  $[\text{M} - 99]^+$ ; HRESIMS  $m/z$ : 390.2281 (calcd for  $\text{C}_{22}\text{H}_{32}\text{NO}_5$ , 390.2280).

## 2.3.5. Parvistemonine F (5)

Yellow amorphous powder;  $[\alpha]_D^{20} - 79$  (c 0.1, Acetone); IR (KBr)  $\nu_{\max}$  2931, 1739, 1680, 1616, 1460, 1398, 1215, 1155, 1063, 1016, and 754  $\text{cm}^{-1}$ ;  $^1\text{H}$  and  $^{13}\text{C}$  NMR data: see Table 3; EIMS  $m/z$  375  $[\text{M}]^+$ , 318, 265, and 208 (100); HRESIMS  $m/z$ : 376.2491 (calcd for  $\text{C}_{22}\text{H}_{34}\text{NO}_4$ , 376.2488).

Table 3.  $^1\text{H}$  (400 MHz) and  $^{13}\text{C}$  NMR (100 MHz) data for compounds 5 in  $\text{CDCl}_3$ .

No.	$\delta_{\text{H}}$	$\delta_{\text{C}}$
1	1.50, m	27.3 t
	1.93, m	
2	1.48, m	30.9 t
	2.01, m	
3	3.03, m	61.1 d
5	3.21, dd (11.7, 4.1)	44.8 t
	2.98, dd (11.7, 7.9)	
6	1.52, m	18.9 t
	1.68, m	
7	1.51, m	33.7 t
	2.34, m	
8	4.13, m	83.8 d
9	2.22, m	56.1 d
9a	3.83, m	58.3 d
10	2.92, m	39.4 d
11		149.1 s
12		124.6 s
13		163.3 s
14		97.1 s
15		170.2 s
16	2.04, s, 3H	9.2 q
17	1.33, d, 3H	20.7 q
18	1.22, m	32.4 t
	1.64, m	
19	1.25, m, 2H	28.4 t
20	1.30, m, 2H	23.0 t
21	0.88, t (7.0), 3H	14.1 q
22-OMe	4.11, s, 3H	58.9 q

### 3. Results

Compound **1** was obtained as light-yellow amorphous powder, positive to Dragendorff's reagent. Its molecular formula was established by HREIMS ( $m/z$  407.2305  $[M]^+$ , calcd 407.2308) as  $C_{22}H_{33}NO_6$  with seven degrees of unsaturation. The  $^1H$  NMR spectrum (Table 1) displayed signals of a methylene ( $\delta_H$  2.87, 3.40) characteristic for the  $CH_2-5$  of the pyrrolo[1,2- $\alpha$ ]azepine nucleus in *Stemona* alkaloids [16], two doublet methyls ( $\delta_H$  1.15, Me-17; 1.25, Me-22), and one singlet methyl ( $\delta_H$  1.50, Me-15). In the  $^{13}C$  NMR spectrum, two quaternary carbons at  $\delta_C$  179.8 and 177.6 suggested the presence of two  $\gamma$ -lactone rings. The base peak at 308  $[M - 99]^+$  in EIMS further confirmed the presence of an  $\alpha$ -methyl- $\gamma$ -lactone moiety attached to C-3 [17,18]. All these data were indicative of a parvistemoline-type skeleton of compound **1**. A further NMR data comparison of compound **1** and the known parvistemonine [11,19] revealed significant similarities of rings A, B, C, and E between these two compounds, except that an oxygenated quaternary carbon ( $\delta_C$  76.1, C-13) and a singlet methyl instead of a doublet methyl in parvistemonine were observed in compound **1**. Considering the molecular formula of **1** contains one more oxygen atom than that of parvistemonine, compound **1** was deduced to be a 13-hydroxyl derivative of parvistemonine. Such elucidation was further confirmed by  $^1H-^1H$  COSY, HSQC, and HMBC spectra (Figures S3–S5). The ROESY correlation between Me-15 and Me-17 suggested an  $\alpha$ -orientation of OH-13 (Figure S6). Therefore, the structure of compound **1** was fully determined and it was named parvistemonine B.

Compound **2**, a yellow amorphous powder, was positive to Dragendorff's reagent. The pseudo-molecular ion at  $m/z$  422.2544 ( $[M + H]^+$ ) in the HRESIMS suggested a molecular formula of  $C_{23}H_{35}NO_6$ , corresponding to seven degrees of unsaturation. Its EIMS base peak at  $m/z$  322 ( $[M - 99]^+$ ) indicated also the existence of an  $\alpha$ -methyl- $\gamma$ -lactone moiety. Further analysis of its NMR data (Tables 1 and 2) revealed that compound **2** was also a parvistemoline-type alkaloid: both the  $^1H$  and  $^{13}C$  NMR data of **2** were quite similar to those of the known parvistemonine and compound **1**, except for the presence of an extra methoxy group ( $\delta_H$  3.35, MeO-23) in **2**, which caused some chemical shift differences at C-12 and C-13. In the  $^{13}C$  NMR and DEPT spectra (Figures S9 and S10), a quaternary carbon signal resonating at  $\delta_C$  110.3 replaced the methine at C-12 in parvistemonine and compound **1**, suggesting the methoxy group might be located at C-12. HMBC correlations from MeO-23, Me-15, and H-16 to C-12 further supported the assumption. The relative configuration of **2** was determined by the NOESY experiment and the cross-peaks of H-11/MeO-23 and H-11/H-13 indicated an  $\alpha$ -orientation of the methoxy group. Therefore, the structure of compound **2** was established and it was named parvistemonine C.

Compound **3** was also obtained as yellow amorphous powder and was positive to Dragendorff's reagent. The molecular formula was established as  $C_{22}H_{33}NO_6$  ( $m/z$  408.2385,  $[M + H]^+$ ) by HRESIMS, with one more oxygen atom than that of parvistemonine. The  $^1H$  NMR data displayed signals of three doublet methyls ( $\delta_H$  1.28–1.30, 9H, overlapped), also indicative of a parvistemonine skeleton. The  $^{13}C$  NMR data highly resembled those of parvistemonine, suggesting that the additional oxygen atom was not substituted at any carbon of the skeleton but at the nitrogen atom. Accordingly, compound **3** was finally proposed as an *N*-oxide derivative of parvistemonine and named parvistemonine D.

The molecular formula of compound **4** was established as  $C_{22}H_{31}NO_5$  according to the pseudo-molecular ion at  $m/z$  390.2281 ( $[M + H]^+$ ) in the HRESIMS and the  $^{13}C$  NMR data, corresponding to eight degrees of unsaturation. Its  $^1H$  NMR data (Table 3) showed the characteristic signals of a methylene ( $\delta_H$  2.99, 2.74), indicative of a pyrrolo[1,2- $\alpha$ ]azepine nucleus (rings A and B). The  $^{13}C$  NMR and DEPT 135 spectra (Table 3, Figures S21–S22) showed resonances ascribed to three methyl, seven methylene, eight methine (one olefinic at  $\delta_C$  147.3 and three oxygenated at  $\delta_C$  71.3, 80.9, and



82.2), and four quaternary carbons (one olefinic at  $\delta_C$  130.6, one oxygenated at  $\delta_C$  105.1, and two carbonyl at  $\delta_C$  173.8 and 179.9). In the EIMS spectrum, the base peak at  $m/z$  290  $[M - 99]^+$  suggested the presence of an  $\alpha$ -methyl- $\gamma$ -lactone moiety. IR absorptions at  $1668\text{ cm}^{-1}$ , together with the carbonyl resonating at  $\delta_C$  173.8, indicated the presence of another  $\alpha,\beta$ -unsaturated  $\alpha$ -methyl- $\gamma$ -lactone ring. The  $^1\text{H}$ - $^1\text{H}$  COSY spectrum (Figure S23) revealed two spin systems of  $-\text{C}(1)\text{H}_2-\text{C}(2)\text{H}_2-\text{C}(3)\text{H}-\text{C}(18)\text{H}-\text{C}(19)\text{H}_2-\text{C}(20)\text{H}-\text{C}(22)\text{H}_3$  and  $-\text{C}(5)\text{H}_2-\text{C}(6)\text{H}_2-\text{C}(7)\text{H}_2-\text{C}(8)\text{H}_2-\text{C}(9)\text{H}-\text{C}(10)\text{H}(\text{CH})-\text{C}(16)\text{H}-\text{C}(17)\text{H}_3$  (Figure 2). The former moiety, in combination with the HMBC correlations from Me-22 and H-19 to the carbonyl carbon (C-21), revealed the  $\alpha$ -methyl- $\gamma$ -lactone (ring E) attached to C-3. HMBC correlations from H-12 and Me-15 to another carbonyl carbon C-14, from H-12 to C-10, and from H-11 to C-16 suggested the  $\alpha,\beta$ -unsaturated lactone ring (ring D) connected to C-10 (Figure 2). Since seven degrees of unsaturation were occupied by the pyrrolo[1,2- $\alpha$ ]azepine nucleus and the identified rings D and E, the remaining one indicated the presence of another ring. Given that C-12 was not oxygenated, together with the obvious down-fielded chemical shifts of C-9a and C-9, the last ring was eventually constructed by forming an oxygen bridge between C-9a and C-16. Therefore, the planar structure of **4** was established.

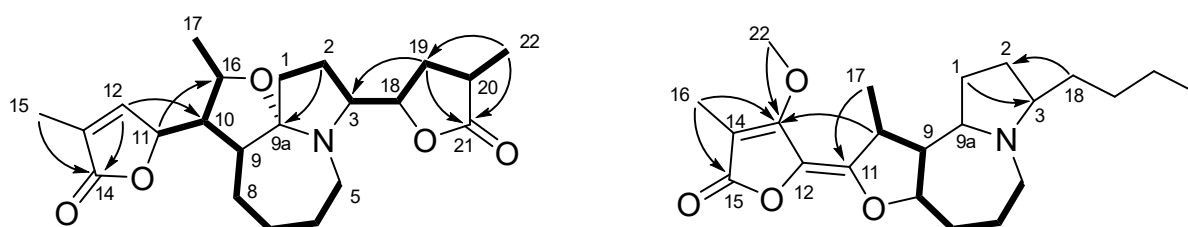


**Figure 2.** Important  $^1\text{H}$ - $^1\text{H}$  COSY (–) and HMBC (H $\rightarrow$ C) correlations of compounds **4** (left) and **5** (right).

The relative configuration was inferred from the NOESY spectrum and biogenetic consideration. The cross-peaks of H-16/H-9 and Me-17/H-10 suggested that the configurations of C-9, C-10, and C-16 could remain untouched. Assuming the configuration at C-11 remained unchanged, there would be two possible configurations for C-9a, as shown in Figure 3. Given the observable correlation between H-16 and H-1, which was only possible when the C-O bond at C-9a was in the  $\alpha$ -orientation, we eventually proposed an *S*-configuration of C-9a.

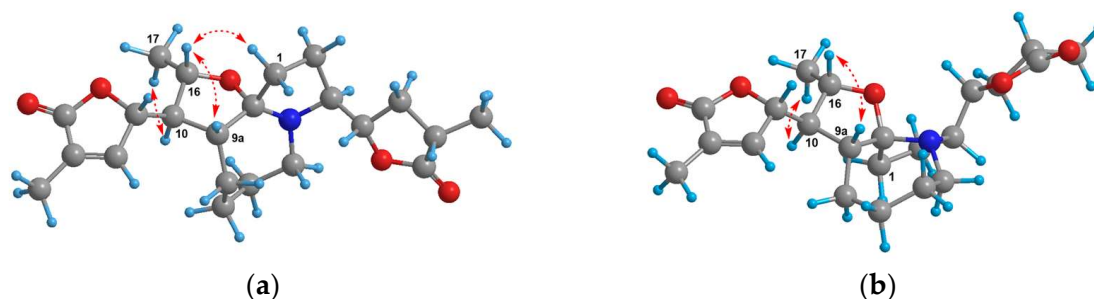


**Figure 3.** 3D structure models of two presumed configurations of compound **4** and key NOESY correlations (H $\leftrightarrow$ H). (a) The C-O bond at C-9a was  $\alpha$ -orientated; (b) the C-O bond at C-9a was  $\beta$ -orientated (generated by ChemBio3D 20.0 software).

The configuration of C-11 was assumed to also be unchanged. However, due to the free rotation caused by the single bond between C-10 and C-11, the relative configuration of C-11 could not be confirmed unambiguously by the NOESY experiment. Therefore,

DFT NMR calculation was performed with the Gaussian 16 program [20] on two possible conformations, 11S-4 and 11R-4 (Figure S29). A conformational search was performed using the Conflex 8.0 software within an energy window of 5.0 kcal/mol [21] and the conformers with a Boltzmann population above 1.0% were selected for re-optimization at the B3LYP/6-31G(d) level in vacuo. The  $^1\text{H}$  and  $^{13}\text{C}$  NMR magnetic shielding tensors of each non-redundant conformer were calculated at the level of mPW1PW91/6-311G(d,p) with the PCM solvent mode for chloroform. The final  $^1\text{H}$  and  $^{13}\text{C}$  NMR data for each conformation were obtained after Boltzmann weighted average. The DP4+ statistical analysis was then used for the experimental and calculated data and the results specified 11S-4 (all data, 100%) as the most probable conformation of **2** (Figure S29) [22].

Subsequently, compound **4** was established as a parvistemoline-type derivative and named parvistemonine E. This structure features a rearranged furan ring, presumably formed through the cleavage of the ether bond of C-12 in parvistemonine, followed by the reformation of a new bond of C-16-O-C-9a. This accounts for the unchanged configurations at C-9, C-10, C-11, and C-16. This type of ring formation is a novel discovery in the *Stemona* alkaloids.

Compound **5**, positive to Dragendorff's reagent, was obtained as a yellow amorphous powder. The HRESIMS data suggested a molecular formula of  $\text{C}_{22}\text{H}_{33}\text{NO}_4$  ( $m/z$  376.2491  $[\text{M} + \text{H}]^+$ ) with an unsaturation equivalence of seven. Considering the fragment peak at  $m/z$  318 ( $[\text{M} - 57]^+$ ) in the EIMS (Figure S37) and a triplet methyl signal ( $\delta_{\text{H}}$  0.88,  $t, J = 7.0$  Hz) in the  $^1\text{H}$  NMR spectrum (Figure S30), an *n*-butyl side chain was proposed. The  $^1\text{H}$  NMR data (Table 3) showed signals of one methoxy ( $\delta_{\text{H}}$  4.11) and three methyls, as well as characteristic signals of the pyrrolo[1,2- $\alpha$ ]azepine nucleus presenting in *Stemona* alkaloids. The  $^{13}\text{C}$  NMR and DEPT 135 spectra (Figures S31 and S32) gave 22 resonances ascribed to four methyls (one methoxy,  $\delta_{\text{C}}$  58.9), eight methylenes, five methines (one oxygenated,  $\delta_{\text{C}}$  83.8), and five quaternary carbons (four olefinic,  $\delta_{\text{C}}$  97.1, 124.6, 149.1, and 163.3; one carboxyl,  $\delta_{\text{C}}$  170.2). The  $^1\text{H}$ - $^1\text{H}$  COSY spectrum (Figure S33) revealed a spin system of  $-\text{C}(5)\text{H}_2-\text{C}(6)\text{H}_2-\text{C}(7)\text{H}_2-\text{C}(8)\text{H}(\text{O})-\text{C}(9)\text{H}-\text{C}(10)\text{H}-\text{C}(17)\text{H}_3$ , which was in accordance with a protostemonine-type skeleton [19]. HMBC correlations from  $\text{H}_3$ -17 to C-11, H-10 to C-12,  $\text{H}_3$ -16 to C-13 and C-15, and OMe-22 to C-13 exhibited an  $\alpha,\beta$ -unsaturated  $\alpha$ -methyl- $\gamma$ -lactone, connecting to ring C through a C11-C12 double bond, while the correlations from H-1 to C-3 and H-18 to C-2 confirmed the *n*-butyl was connecting to C-3. All these data evidenced that the structure of compound **5** closely resembled that of protostemonine with the exception of an *n*-butyl group being present instead of an  $\alpha$ -methyl- $\gamma$ -lactone group at C-3. The relative configuration was fixed by the NOESY experiment. The correlations of Me-17/H-9 and H-10/H-8 suggested that Me-17 and H-9 were on the same face, and they were designated as  $\beta$  based on biogenetic consideration, while H-10 and H-8 were on the other face and  $\alpha$ -oriented. The correlation observed between H-3 and H-8 suggested that it was indicative of the specific configuration where H-9a was in the  $\beta$  orientation, while H-3 and H-8 were both in the  $\alpha$  orientation. This observation conclusively established the relative configuration of H-9a and H-3. Consequently, the structure of compound **5** was fully elucidated. Considering the *n*-butyl side chain was distinct in stemofoline-type alkaloids [23], compound **5** was named parvistemonine F.

Accompanying the new compounds, eight known alkaloids were identified, parvistemonine [11], parvineostemonine [8], protostemonine [18], croomine [2], protostemoamide [24], stemofoline [23], maistemonine [25], and isomaistemonine [26], by comparison with data in the literature.



## 4. Discussion

*Stemona* alkaloids are a small family of unique structures that have a pyrrolo[1,2- $\alpha$ ]azepine or a pyrido[1,2- $\alpha$ ]azepine nucleus. Based on their structural features, the classification of these alkaloids was presented firstly by Götz and Strunz in 1975 [27]. Then, Pilli et al. proposed in 2000 and 2010 to classify *Stemona* alkaloids into six or eight structural groups, respectively [14,15]. In this paper, we have followed the aforementioned classification method, categorizing the obtained compounds 1–4 as parvistemoline-type compounds. This classification method effectively reflects the structural characteristics of the compounds but lacks a description of the biosynthetic relationships between different structural types.

In 2006, Greger suggested a new classification based on biosynthetic considerations and classified the *Stemona* alkaloids into three skeletal types—the stichoneurine-type (tuberostemonine-type), protostemonine-type, and croomine-type alkaloids—according to the different carbon chains attached to C-9 of the pyrroloazepine nucleus [4,28]. In his classification, parvistemoline-type alkaloids were eventually classified as stemonine-type derivatives of the stichoneurine skeleton [4]. The structure of parvistemoline is hypothesized to originate from the formation of an ether linkage between C-12 and C-16 of a stichoneurine-type compound. The structure of compound 4, which constructs an ether linkage between C-9a and C-16, further supported the hypothesis that the stichoneurine-type served as a common precursor for both parvistemoline and parvistemonine E (4), effectively accounting for the cooccurrence of these two compounds (Figure 4).

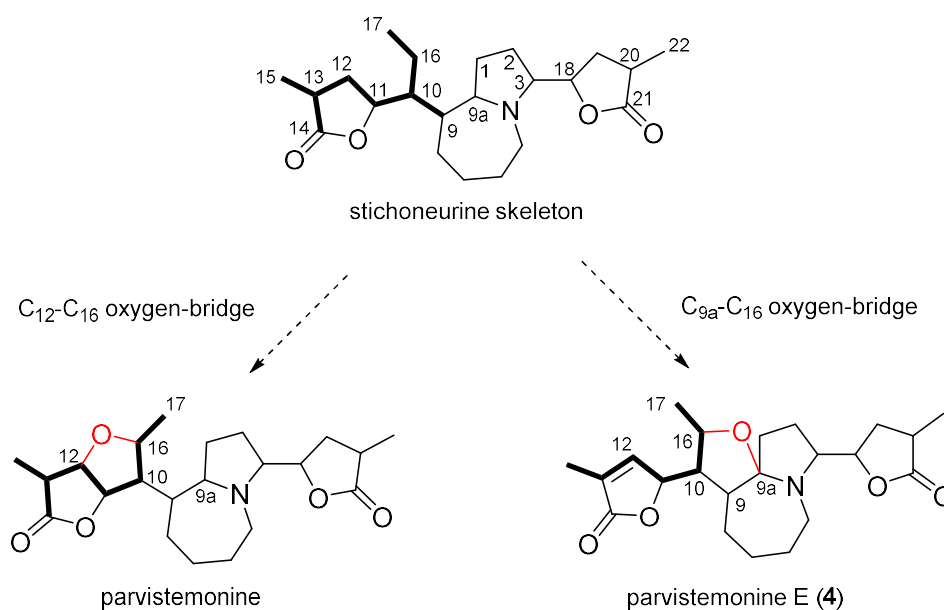


**Figure 4.** Proposed biosynthetic pathway from the stichoneurine skeleton to parvistemonine and parvistemonine E (4) through a C<sub>12</sub>-C<sub>16</sub> or a C<sub>9a</sub>-C<sub>16</sub> oxygen bridge, respectively.

## 5. Conclusions

In this study, we successfully isolated five new alkaloids from the roots of *S. parviflora*. Among these, four compounds (1–4) are derivatives of the parvistemoline-type alkaloids, a relatively rare class of structures reported in previous phytochemical investigations of *Stemona* species. Notably, compound 4 represents the first identified ring-C rearranged skeleton within this group of compounds. In addition, compound 5 possesses a unique structural skeleton, representing a hybrid protostemonine-type and stemofoline-type compound. Our findings expand the chemical diversity of *S. parviflora* and provide valuable clues for the study of the biosynthetic pathways of *Stemona* alkaloids.

**Supplementary Materials:** The following supporting information can be downloaded at: <https://www.mdpi.com/article/10.3390/chemistry7010006/s1>, Supplementary data for *Stemona parviflora*: Figure S1.  $^1\text{H}$  NMR spectrum of compound **1** (300 MHz,  $\text{CDCl}_3$ ); Figure S2.  $^{13}\text{C}$  NMR and DEPT 135 spectrum of compound **1** (100 MHz,  $\text{CDCl}_3$ ); Figure S3.  $^1\text{H}$ - $^1\text{H}$  COSY spectrum of compound **1** (400 MHz,  $\text{CDCl}_3$ ); Figure S4. HSQC spectrum of compound **1** (400 MHz,  $\text{CDCl}_3$ ); Figure S5. HMBC spectrum of compound **1** (400 MHz,  $\text{CDCl}_3$ ); Figure S6. ROESY spectrum of compound **1** (500 MHz,  $\text{CDCl}_3$ ); Figure S7. HREIMS spectrum of compound **1**; Figure S8.  $^1\text{H}$  NMR spectrum of compound **2** (300 MHz,  $\text{CDCl}_3$ ); Figure S9.  $^{13}\text{C}$  NMR spectrum of compound **2** (100 MHz,  $\text{CDCl}_3$ ); Figure S10. DEPT 135 spectrum of compound **2** (100 MHz,  $\text{CDCl}_3$ ); Figure S11.  $^1\text{H}$ - $^1\text{H}$  COSY (400 MHz,  $\text{CDCl}_3$ ) spectrum of compound **2**; Figure S12. HSQC spectrum of compound **2** (400 MHz,  $\text{CDCl}_3$ ); Figure S13. HMBC spectrum of compound **2** (400 MHz,  $\text{CDCl}_3$ ); Figure S14. NOESY spectrum of compound **2** (500 MHz,  $\text{CDCl}_3$ ); Figure S15. EIMS spectrum of compound **2**; Figure S16. HRESIMS spectrum of compound **2**; Figure S17.  $^1\text{H}$  NMR spectrum of compound **3** (300 MHz,  $\text{CDCl}_3$ ); Figure S18.  $^{13}\text{C}$  NMR spectrum of compound **3** (100 MHz,  $\text{CDCl}_3$ ); Figure S19. HRESIMS spectrum of compound **3**; Figure S20.  $^1\text{H}$  NMR spectrum of compound **4** (300 MHz,  $\text{CDCl}_3$ ); Figure S21.  $^{13}\text{C}$  NMR spectrum of compound **4** (100 MHz,  $\text{CDCl}_3$ ); Figure S22. DEPT 135 spectrum of compound **4** (100 MHz,  $\text{CDCl}_3$ ); Figure S23.  $^1\text{H}$ - $^1\text{H}$  COSY spectrum of compound **4** (400 MHz,  $\text{CDCl}_3$ ); Figure S24. HSQC spectrum of compound **4** (400 MHz,  $\text{CDCl}_3$ ); Figure S25. HMBC spectrum of compound **4** (400 MHz,  $\text{CDCl}_3$ ); Figure S26. NOESY spectrum of compound **4** (500 MHz,  $\text{CDCl}_3$ ); Figure S27. EIMS spectrum of compound **4**; Figure S28. HRESIMS spectrum of compound **4**; Figure S29. DFT NMR calculations performed on compound **4**. (a) Two possible conformations, 11S-4 (Isomer 1) and 11R-4 (Isomer 2); (b) DP4+ probability analysis result for compound **4**; Figure S30.  $^1\text{H}$  NMR spectrum of compound **5** (400 MHz,  $\text{CDCl}_3$ ); Figure S31.  $^{13}\text{C}$  NMR spectrum of compound **5** (100 MHz,  $\text{CDCl}_3$ ); Figure S32. DEPT 135 spectrum of compound **5** (100 MHz,  $\text{CDCl}_3$ ); Figure S33.  $^1\text{H}$ - $^1\text{H}$  COSY spectrum of compound **5** (400 MHz,  $\text{CDCl}_3$ ); Figure S34. HSQC spectrum of compound **5** (400 MHz,  $\text{CDCl}_3$ ); Figure S35. HMBC spectrum of compound **5** (400 MHz,  $\text{CDCl}_3$ ); Figure S36. NOESY spectrum of compound **5** (500 MHz,  $\text{CDCl}_3$ ); Figure S37. EIMS spectrum of compound **5**; Figure S38. HRESIMS spectrum of compound **5**.

**Author Contributions:** Conceptualization, C.T. and Y.Y.; methodology, C.K.; software, C.T.; validation, S.Z., F.G. and C.T.; formal analysis, S.Z.; investigation, S.Z., R.G. and F.G.; resources, Y.C.; data curation, C.T.; writing—original draft preparation, S.Z.; writing—review and editing, C.T.; visualization, R.G. and Y.C.; supervision, Y.Y.; project administration, C.T.; funding acquisition, Y.Y. All authors have read and agreed to the published version of the manuscript.

**Funding:** This research was funded by the Key-Area Research and Development Program of Guangdong Province (2020B0303070002) and the National Key R&D Program “Strategic Scientific and Technological Innovation Cooperation” Key Project (2022YFE0203600) released by the Ministry of Science and Technology of China.

**Data Availability Statement:** The original contributions presented in this study are included in the article/Supplementary Material. Further inquiries can be directed to the corresponding author(s).

**Conflicts of Interest:** The authors declare no conflicts of interest. The funders had no role in the design of the study; in the collection, analyses, or interpretation of data; in the writing of the manuscript; or in the decision to publish the results.

## References

1. Lu, R.; Xu, W.; Lu, Q.; Li, P.; Losh, J.; Hina, F.; Li, E.; Qiu, Y. Generation and classification of transcriptomes in two *Croomia* species and molecular evolution of *CYC/TB1* genes in *Stemonaceae*. *Plant Divers.* **2018**, *40*, 253–264. [[CrossRef](#)] [[PubMed](#)]
2. Jiang, R.W.; Hon, P.M.; Xu, Y.T.; Chan, Y.M.; Xu, H.X.; Shaw, P.C.; But, P.P.H. Isolation and chemotaxonomic significance of tuberostemospironine-type alkaloids from *Stemona tuberosa*. *Phytochemistry* **2006**, *67*, 52–57. [[CrossRef](#)] [[PubMed](#)]
3. Liu, Y.Q.; Shen, Y.; Teng, L.; Yang, L.F.; Cao, K.; Fu, Q.; Zhang, J.L. The traditional uses, phytochemistry, and pharmacology of *Stemona* species: A review. *J. Ethnopharmacol.* **2021**, *265*, 113112. [[CrossRef](#)] [[PubMed](#)]
4. Greger, H. Structural classification and biological activities of *Stemona* alkaloids. *Phytochem. Rev.* **2019**, *18*, 463–493. [[CrossRef](#)]

5. Nguyen-Thi, C.; Vo-Cong, D.; Giang, L.D.; Dau-Xuan, D. Isolation and bioactivities of *Stemona* Alkaloid: A review. *Nat. Prod. Commun.* **2024**, *19*, 1–26. [[CrossRef](#)]
6. Zhang, X.; Ge, J.; Yang, J.; Dunn, B.; Chen, G. Genetic diversity of *Stemona parviflora*: A threatened myrmecochorous medicinal plant in China. *Biochem. Syst. Ecol.* **2017**, *71*, 193–199. [[CrossRef](#)]
7. Huang, S.Z.; Kong, F.D.; Ma, Q.Y.; Guo, Z.K.; Zhou, L.M.; Wang, Q.; Dai, H.F.; Zhao, Y.X. Nematicidal *Stemona* alkaloids from *Stemona parviflora*. *J. Nat. Prod.* **2016**, *79*, 2599–2605. [[CrossRef](#)]
8. Ke, C.Q.; He, Z.S.; Yang, Y.P.; Ye, Y. A novel alkaloid from *Stemona parviflora*. *Chin. Chem. Lett.* **2003**, *14*, 173–175.
9. Lin, W.H.; Xu, R.S.; Zhong, Q.X. Chemical studies on *Stemona* alkaloids. I. Studies on new alkaloids of *Stemona parviflora* C. H. Wright. *Acta Chim. Sin.* **1991**, *49*, 927–931.
10. Lin, W.H.; Xu, R.S.; Zhong, Q.X. Chemical studies on *Stemona* alkaloids. II. Studies on the minor alkaloids of *Stemona parviflora* Wright C. H. *Acta Chim. Sin.* **1991**, *49*, 1034–1037.
11. Lin, W.H.; Yin, B.P.; Tang, Z.J.; Xu, R.S.; Zhong, Q.X. The structure of parvistemonine. *Acta Chim. Sin.* **1990**, *48*, 811–814.
12. Yang, X.Z.; Gulder, T.A.A.; Reichert, M.; Tang, C.P.; Ke, C.Q.; Ye, Y.; Bringmann, G. Parvistemins A–D, a new type of dimeric phenylethyl benzoquinones from *Stemona parviflora* Wright. *Tetrahedron* **2007**, *63*, 4688–4694. [[CrossRef](#)]
13. Huang, S.Z.; Kong, F.D.; Chen, G.; Cai, X.H.; Zhou, L.M.; Ma, Q.Y.; Wang, Q.; Mei, W.L.; Dai, H.F.; Zhao, Y.X. A phytochemical investigation of *Stemona parviflora* roots reveals several compounds with nematocidal activity. *Phytochemistry* **2019**, *159*, 208–215. [[CrossRef](#)]
14. Pilli, R.A.; de Oliveira, M.D.C.F. Recent progress in the chemistry of the *Stemona* alkaloids. *Nat. Prod. Rep.* **2000**, *17*, 117–127. [[CrossRef](#)] [[PubMed](#)]
15. Pilli, R.A.; Rosso, G.B.; de Oliveira, M.D.F. The chemistry of *Stemona* alkaloids: An update. *Nat. Prod. Rep.* **2010**, *27*, 1908–1937. [[CrossRef](#)] [[PubMed](#)]
16. Ye, Y.; Qin, G.W.; Xu, R.S. Alkaloids of *Stemona japonica*. *J. Nat. Prod.* **1994**, *57*, 655–669. [[CrossRef](#)]
17. Xu, R.S.; Lu, Y.J.; Chu, J.H.; Iwashita, T.; Naoki, H.; Naya, Y.; Nakanishi, K. Studies on some new *Stemona* alkaloids—A diagnostically Useful <sup>1</sup>H-NMR line-broadening effect. *Tetrahedron* **1982**, *38*, 2667–2670. [[CrossRef](#)]
18. Ye, Y.; Xu, R.S. Studies on new alkaloids of *Stemona japonica*. *Chin. Chem. Lett.* **1992**, *3*, 511–514.
19. Kaltenecker, E.; Brem, B.; Mereiter, K.; Kalchauer, H.; Kählig, H.; Hofer, O.; Vajrodaya, S.; Greger, H. Insecticidal pyrido[1,2- $\alpha$ ]azepine alkaloids and related derivatives from *Stemona* species. *Phytochemistry* **2003**, *63*, 803–816. [[CrossRef](#)]
20. Frisch, M.J.; Trucks, G.W.; Schlegel, H.B.; Scuseria, G.E.; Robb, M.A.; Cheeseman, J.R.; Scalmani, G.; Barone, V.; Petersson, G.A.; Nakatsuji, H.; et al. *Gaussian 16, Revision C.01*; Gaussian, Inc.: Wallingford, CT, USA, 2016.
21. Goto, H.; Obata, S.; Kakayama, N.; Ohta, K. *CONFLEX 8*; CONFLEX Corporation: Tokyo, Japan, 2017.
22. Zanardi, M.M.; Sarotti, A.M. Sensitivity Analysis of DP4+ with the Probability Distribution Terms: Development of a Universal and Customizable Method. *J. Org. Chem.* **2021**, *86*, 8544–8548. [[CrossRef](#)]
23. Irie, H.; Masaki, N.; Ohno, K.; Osaki, K.; Taga, T.; Uyeo, S. The crystal structure of a new alkaloid, stemofoline, from *Stemona japonica*. *J. Chem. Soc. D* **1970**, *17*, 1066. [[CrossRef](#)]
24. Yang, X.Z.; Zhu, J.Y.; Tang, C.P.; Ke, C.Q.; Lin, G.; Cheng, T.Y.; Rudd, J.A.; Ye, Y. Alkaloids from roots of *Stemona sessilifolia* and their antitussive activities. *Planta Med.* **2009**, *75*, 174–177. [[CrossRef](#)] [[PubMed](#)]
25. Lin, W.H.; Ye, Y.; Xu, R.S. Studies on new alkaloids of *Stemona mairei*. *Chin. Chem. Lett.* **1991**, *2*, 369–370.
26. Guo, A.; Jin, L.; Deng, Z.; Cai, S.; Guo, S.; Lin, W. New *Stemona* alkaloids from the roots of *Stemona sessilifolia*. *Chem. Biodiver.* **2008**, *5*, 598–605. [[CrossRef](#)]
27. Götz, M.; Strunz, G.M. Tuberosstemonine and Related Compounds: The Chemistry of *Stemona* Alkaloids. In *Alkaloids*; Wiesner, G., Ed.; Butterworths: London, UK, 1975; Volume 9, pp. 143–160.
28. Greger, H. Structural relationships, distribution and biological activities of *Stemona* alkaloids. *Planta Med.* **2006**, *72*, 99–113. [[CrossRef](#)]

**Disclaimer/Publisher’s Note:** The statements, opinions and data contained in all publications are solely those of the individual author(s) and contributor(s) and not of MDPI and/or the editor(s). MDPI and/or the editor(s) disclaim responsibility for any injury to people or property resulting from any ideas, methods, instructions or products referred to in the content.